Application of Degradation Kinetics to the Rheology of Poly(hydroxyalkanoates)

Graham M. Harrison,[1] David H. Melik[2]

[1]*Department of Chemical Engineering and Center for Advanced Engineering Fibers and Films, Clemson University, Clemson, South Carolina 29634*
[2]*The Procter and Gamble Company, Beckett Ridge Technical Center, West Chester, Ohio 45069*

Received 8 June 2005; accepted 17 January 2006
DOI 10.1002/app.24473
Published online in Wiley InterScience (www.interscience.wiley.com).

ABSTRACT: The time-dependent rheological behavior of a series of 3-hydroxybuytrate-based semicrystalline copolymers is employed to determine the expected rheological curves that would be generated in the absence of any polymer degradation. Both dynamic frequency sweep and shear rate sweep experiments were analyzed. A model for the degradation kinetics, coupled with standard rheological relationships, was employed to extrapolate the measured sweeps to predicted curves at time zero, prior to degradation. The model is broadly applicable over a wide range of frequencies or shear rates, and generates a single degradation rate constant k for each polymer studied. A similar, although *ad hoc*, procedure was applied to the dynamic storage and loss moduli. The model provides a method for determining the rheological behavior of degrading polymers over a time interval, typically found in processing applications. © 2006 Wiley Periodicals, Inc. J Appl Polym Sci 102: 1794–1802, 2006

Key words: polymer degradation; rheology; kinetics; PHA

INTRODUCTION

The class of polymers known as poly(hydroxyalkanoates) (PHAs) has attracted widespread attention in literature,[1–14] in part because of the wide range of copolymers that can be produced and the subsequent breadth of potential commercial applications. In addition to conventional synthetic routes of production, there are a variety of biologically based synthesis processes available. It is these biologically derived polymers that offer an alternative to conventional, petroleum-derived materials.

Biopol, developed by ICI and produced by Metabolix, was the first commercially available PHA.[4] Recently, Procter and Gamble has introduced the Nodax™ family of PHAs, which is based upon 3-hydroxybutyrate (3HB) with a comonomer type and concentration that can be manipulated.[14] Depending on the specific polymer architecture chosen, these materials have the potential to match conventional petroleum-based polymer mechanical properties to be suitable for a wide range of commodity polymer applications. In addition, there are significant potential benefits to the environment because of both the feedstock of the materials and the degradability under aerobic or anaerobic conditions.[3,6]

One of the potential drawbacks of PHA materials is that they can degrade at temperatures typical of many processing applications. Therefore, to understand and predict the properties of a prospective PHA product, it is imperative to have an understanding of the polymer molecular weight and flow properties of the polymer as a function of time and of thermal history, as well as a detailed knowledge of the thermal environment encountered during the processing itself. With all of this information, appropriate steps can be taken to ensure that the necessary molecular weight for the proposed application can be achieved at the end of processing.

Rheological testing is employed to evaluate the flow properties of a material in a relatively simple, well-controlled flow geometry. These flow experiments enable one to determine the material properties of the polymer, such as the shear viscosity η, as a function of shear rate, and the storage (G') and loss (G'') moduli as a function of frequency. In addition, rheological measurements can be used to quantify polymer characteristics, such as a characteristic relaxation time or the molecular weight between entanglements. All of these measurements may be used to determine whether a specified polymer will be appropriate for a particular application, to understand how that polymer will flow in a specific processing

Correspondence to: G. M. Harrison (graham.harrison@ces.clemson.edu).

Contract grant sponsor: The National Science Foundation; contract grant number: EEC-9731680.

TABLE I
Properties of the Copolymers Employed in This Study

Polymer	Comonomer level (mol %)	M_w	M_w/M_n	T_m (°C)
3HB-3HV	10.5	631K	2.57	156
3HB-3HH	6	765K	1.47	132
3HB-6HH	17	458K	1.62	125

geometry, and to help determine the final properties of a processed material.

Rheological measurements are strongly dependent both on polymer structure and on molecular weight. Because PHAs can degrade at typical processing or melt rheological test temperatures, it can be difficult to interpret rheological measurements for these materials, because they are a strong function of time. Prior work[15] has demonstrated how a combined rheology/GPC study can be used to determine the degradation kinetics of a polymer, by measuring the change in complex viscosity (at a particular frequency) as a function of time, and correlating that result with measurements of the time-dependent molecular weight. A related research question is how to determine the complete flow curve as a function of shear rate or frequency in a manner that can account for the degradation that occurs during the time window, required to complete the flow experiment.

In this work, we investigate the flow behavior of a series of PHAs. Both steady shear rate sweep experiments and dynamic oscillatory frequency sweep experiments are performed. In a single experimental run, the degradation of the polymer is measured by repeating the sweep four times. Using a kinetic model for random polymer degradation,[14–17] the expected rheological curves that would occur in the absence of degradation are determined. An evaluation of the Cox–Merz rule[18] under these conditions is performed. While this article focuses on PHA material, the technique described may be applied to a range of polymer systems that may degrade during rheological testing.

Theory

In this section, we outline the theoretical underpinnings of the method by which we employ time-dependent rheological measurements and degradation theory to determine the flow curves in the absence of degradation. PHAs have been shown to undergo random thermal degradation.[1,19] For a polymer system undergoing random degradation, the change in molecular weight M_w as a function of time can be expressed by[16]

$$\frac{1}{M_{w,0}} - \frac{1}{M_w} = -\frac{k}{2M_0}t \tag{1}$$

where $M_{w,0}$ is the initial weight average molecular weight, M_0 is the molecular weight of the polymer repeat unit, and k is the thermal degradation rate constant. In rheological experiments, the complex viscosity $\eta^*(\omega)$ for highly entangled polymer melts can be related to the molecular weight of the polymer under investigation through

$$\eta^* = KM_w^{\alpha(\omega)} \tag{2}$$

where K is a material constant and $\alpha(\omega)$ is a power law exponent. The empirical frequency dependent power law exponent has a form given by[8]

$$\alpha = \frac{\alpha_0}{\left(1 + (b_1\omega)^{b_2}\right)} \tag{3}$$

where α_0 is the standard zero-shear rate power law exponent and b_1 and b_2 are material dependent constants. As is common, we will take $\alpha_0 = 3.4$.

By substituting eq. (2) into eq. (1), we obtain an expression that, for a given frequency, describes the viscosity as a function of time and polymer degradation:

$$\left(\frac{\eta^*(\omega)\big|_{t=0}}{\eta^*(\omega, t)}\right)^{1/\alpha} = 1 + \left(\frac{kM_{w,0}}{2M_0}\right)t. \tag{4}$$

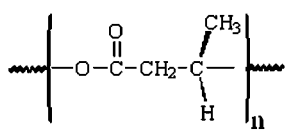

(a)

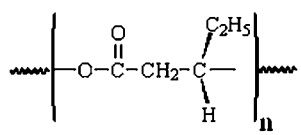

(b)

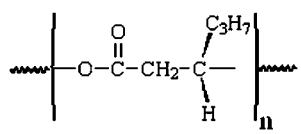

(c)

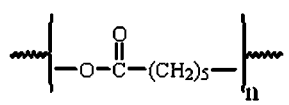

(d)

Figure 1 Structures of the monomers employed in this study. (a) 3-HB; (b) 3-hydroxyvalerate; (c) 3-hydroxyhexanoate; (d) 6-hydroxyhexanoate.

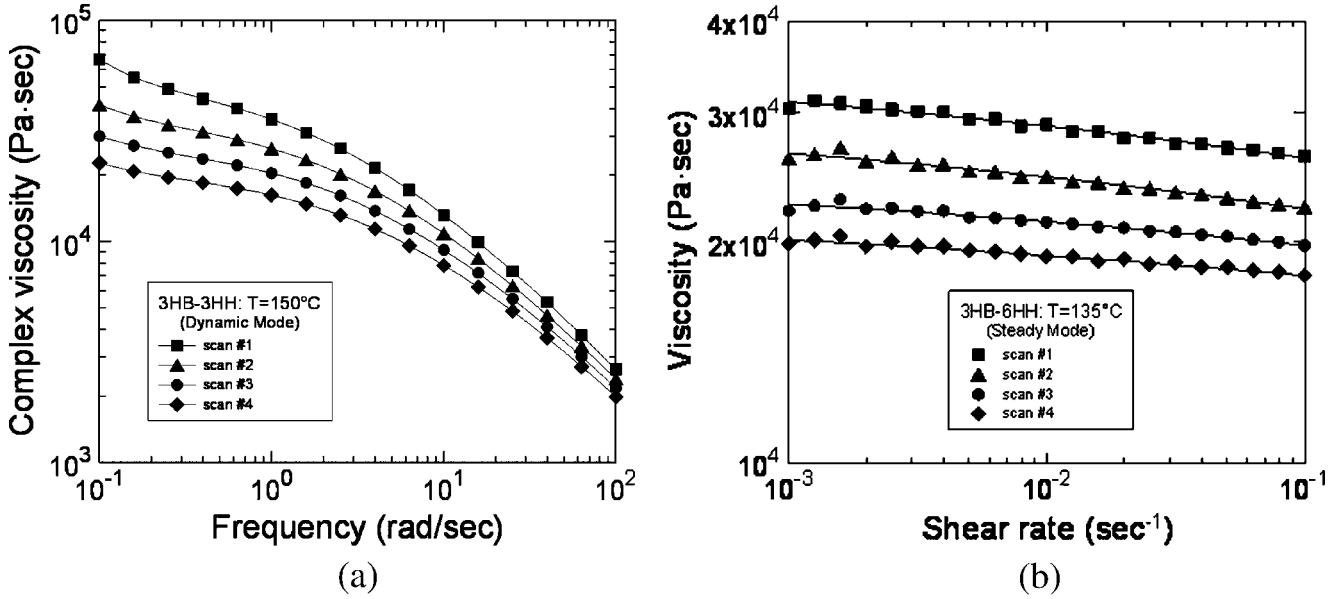

Figure 2 (a) Sequential complex viscosity–frequency sweeps for a 3HB-3HH copolymer; (b) Sequential shear viscosity-shear rate sweeps for a 3HB-6HH copolymer.

Experimentally, we can measure the complex viscosity $\eta^*(\omega,t)$, and our goal is to the determine the initial, time zero, viscosity $\eta^*(\omega)\,|_{\,t\,=\,0}$, prior to degradation. Because $\alpha(\omega)$ is generally unknown, we can expand eq. (4) in a series around $t = 0$ and obtain

$$\log \eta^*(\omega,t) = \log \eta^*(\omega)|_{t=0} - \alpha\left(\frac{kM_{w,0}}{2M_0}\right)t + \frac{\alpha}{2}\left(\frac{kM_{w,0}}{2M_0}\right)^2 t^2 - \mathrm{O}(t^3). \quad (5)$$

Rewriting eq. (5) in a more compact form, we can say

$$\log \eta^*(\omega,t) = \log \eta^*(\omega)|_{t=0} + \sum_{i=1}^{\infty}(-1)^i(R_{\mathrm{vi}}t^i) \quad (6)$$

where R_{vi} is an ith-order viscosity loss rate defined by

$$R_{\mathrm{vi}} = \frac{\alpha}{i}\left(\frac{kM_{w,0}}{2M_0}\right)^i. \quad (7)$$

Given a knowledge of the polymer characteristics, and a series of viscosity–frequency (or shear rate) sweeps as a function of (known) time, it is therefore possible to determine the initial viscosity curve over a range of frequency (shear rate) that would be measured prior to any degradation that occurs.

Equation (6) is based upon the complex viscosity $\eta^*(\omega)$. An analogous expression may be obtained for steady shear rate sweeps by replacing the frequency ω with the shear rate $\dot{\gamma}$. In addition, an analogous expression to eq. (4) may be developed for materials that undergo both thermal and hydrolytic degradation[20] by adding in an additional term for the hydrolytic degradation.

MATERIALS AND METHODS

Three semicrystalline PHA polymers were employed in this study. All of the polymers are copolymers based upon 3-hydroxybutyrate (3HB). The polymer molecular weights and architectures are described in Table I. The 3HB-3HV copolymer was produced by

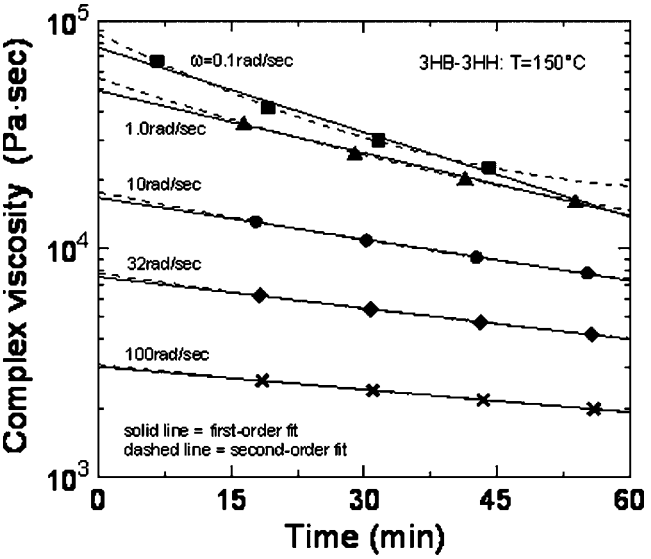

Figure 3 First- and second-order fits of the complex viscosity–time data at five representative frequencies for the 3HB-3HH copolymer.

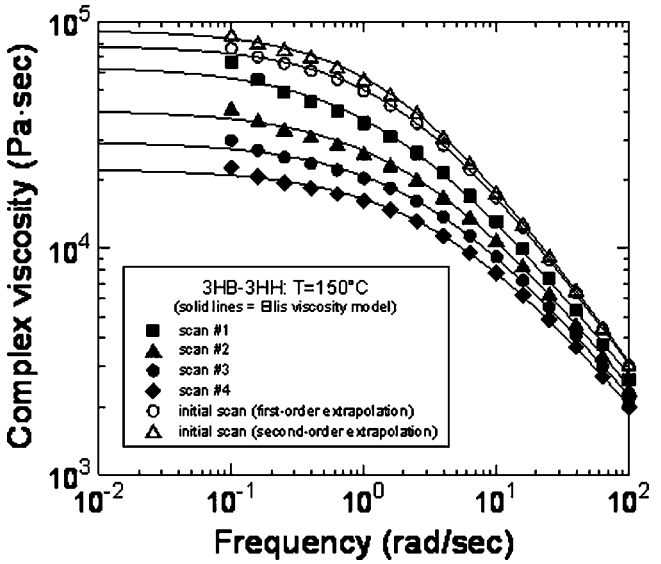

Figure 4 First-and second-order extrapolated complex viscosity–frequency curves for the 3HB-3HH copolymer.

bacterial fermentation and is isotactic, whereas the 3HB-3HH and 3HB-6HH copolymers were produced synthetically and are largely, but not completely isotactic.[14] Structures of the monomers are shown in Figure 1. The copolymers incorporating 3HV and 3HH differ in the length of the alkyl sidegroup in the comonomer. The copolymer that incorporates 6HH has a longer alkyl group that contributes to the polymer backbone and is likely to be more flexible.

Samples for the rheological experiments were prepared by compression molding of the polymer into 1.5-mm thick sheets at temperatures ~10°C above the melting temperature. After cooling the sheets, disks of 27 mm diameter were cut. The samples were then stored in a vacuum oven overnight at 60°C before the experiments were performed.

Rheological results were obtained using a Rheometrics Dynamic Analyzer RDA-II fitted with 25-mm diameter parallel plates. Both dynamic frequency sweeps and steady shear rate sweeps were performed. For each sample, four sequential sweeps were conducted to observe how the measured viscosity decreased with increasing time. For all experiments, a nitrogen atmosphere was used.

Because time is such a critical parameter in the theoretical methodology employed, a consistent experimental protocol was followed for each experiment performed. The plates were first equilibrated at the test temperature in the rheometer furnace followed by zeroing the gap. After zeroing, the gap was set to 3 mm, and the furnace was opened. As the polymer sample disk was inserted and the furnace closed to heat the sample, a stopwatch was started to track elapsed time. An initial gap was set, and the sample melted in the furnace. After 1 min, the furnace was opened to trim excess material from the plates. The furnace was closed again, and the gap reduced to the test position. The sample was allowed to equilibrate, and then the experiments were begun. For all experiments, time equal to zero (e.g. $t = 0$) was measured from when the stopwatch was started after the sample was initially loaded between the plates.

For the dynamic frequency sweep experiments, all experiments were conducted in the linear viscoelastic regime, and the frequency was varied from 0.1 to 100 rad/s. For the steady shear rate sweep experiments, the appropriate delay before each measurement time was determined to be 15 s, and a measurement interval of 15 s was sufficient to minimize noise in the results. Shear rates ranged from 0.001 to 0.1 s^{-1}.

RESULTS AND DISCUSSION

In Figure 2(a), we present representative complex viscosity–frequency sweeps as a function of time, in this case for the 3HB-3HH copolymer. At low frequencies, the complex viscosity approaches a constant (zero-shear) value. As the frequency increases in each scan, we observe shear-thinning due primarily to polymer orientation. The second scan was performed at the conclusion of the complete first scan frequency sweep. Owing to the degradation of the polymer[15] and the decrease in the polymer molecular weight, we observe that the second (and subsequently the third and the fourth) scans show a continual decrease in the measured complex viscosity (at equivalent frequencies). Therefore, the flow curves

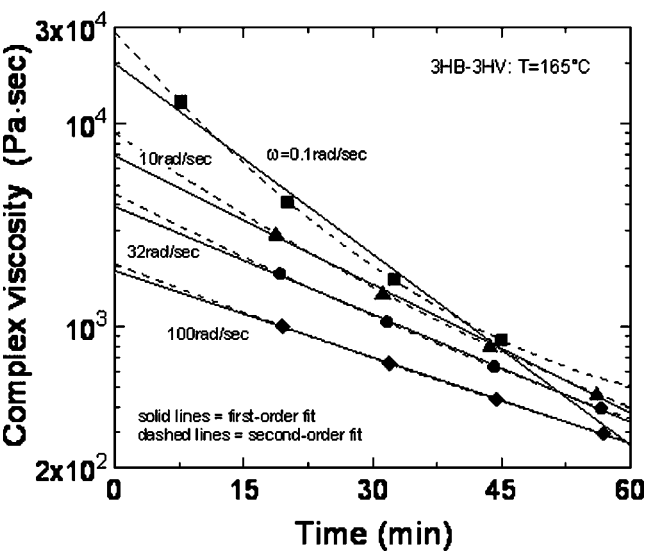

Figure 5 First- and second-order fits of the complex viscosity–time data at five representative frequencies for the 3HB-3HV copolymer.

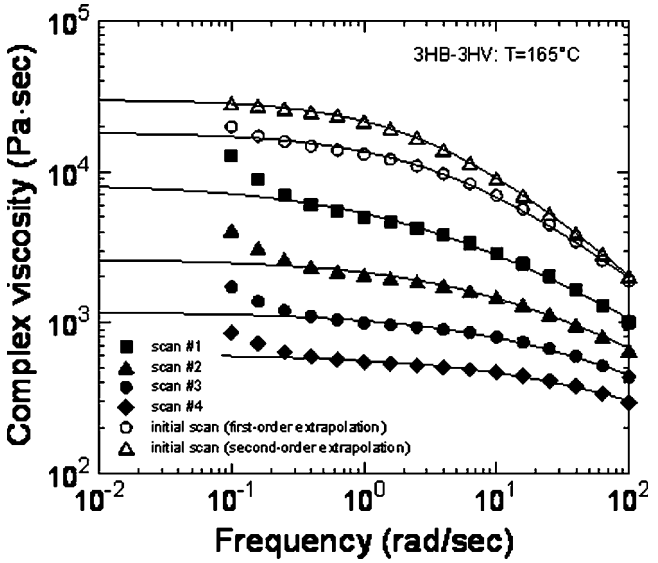

Figure 6 First-and second-order extrapolated complex viscosity–frequency curves for the 3HB-3HV copolymer.

shown are a result of both polymer orientation and shear thinning.

Figure 2(b) shows the curves for the steady shear rate sweep experiment for the 3HB-6HH copolymer. Because the shear rates reported are lower than those frequencies encountered in the frequency sweep experiment, the viscosity does not show dramatic shear thinning, although there is a small but noticeable decrease in the viscosity with increasing shear rate. However, we attribute this decrease not to shear thinning effects associated with polymer orientation, but rather due to the time required to conduct this experiment. If one looks at the viscosity measured at the upper shear rates probed (10^{-1} s^{-1}) for the first scan, it is almost identical to that measured at the lowest shear rate (10^{-3} s^{-1}) for the second scan. Experimentally, these points are measured sequentially (the time between measurements is described in the previous section). Therefore, we believe that the decrease in viscosity observed in Figure 2(b) is due to the degradation of the polymer with time and is not due to shear-thinning effects.

Given the types of curves produced experimentally and shown in Figure 2, we now apply the theoretical framework outlined earlier to obtain the expected viscosity curves that would occur at time equal to zero, if we were able to measure the viscosity in the absence of any degradation.

Complex viscosity

In Figure 3, five representative frequencies are chosen from the 3HB-3HH experiment shown in Figure 2(a), and the complex viscosity is plotted as a function of time (as defined in the experimental methods section). As expected, the low frequency values take the most time to measure whereas, at high frequencies, the required oscillation to obtain the value occurs very rapidly. Figure 3 also shows the results for the first- and second-order extrapolation method of eq. (6). At high frequencies, both methods seem to provide suitable fits to the experimental data. However, at the lower frequencies, it is apparent that the second order extrapolation method provides a better fit to the time-dependent data. Higher order fits are generally not justified, since the results are usually not statistically different from the second-order fits.

Figure 4 shows the complex viscosity–frequency curves for the 3HB-3HH copolymer, including the calculated extrapolated curves (in the absence of

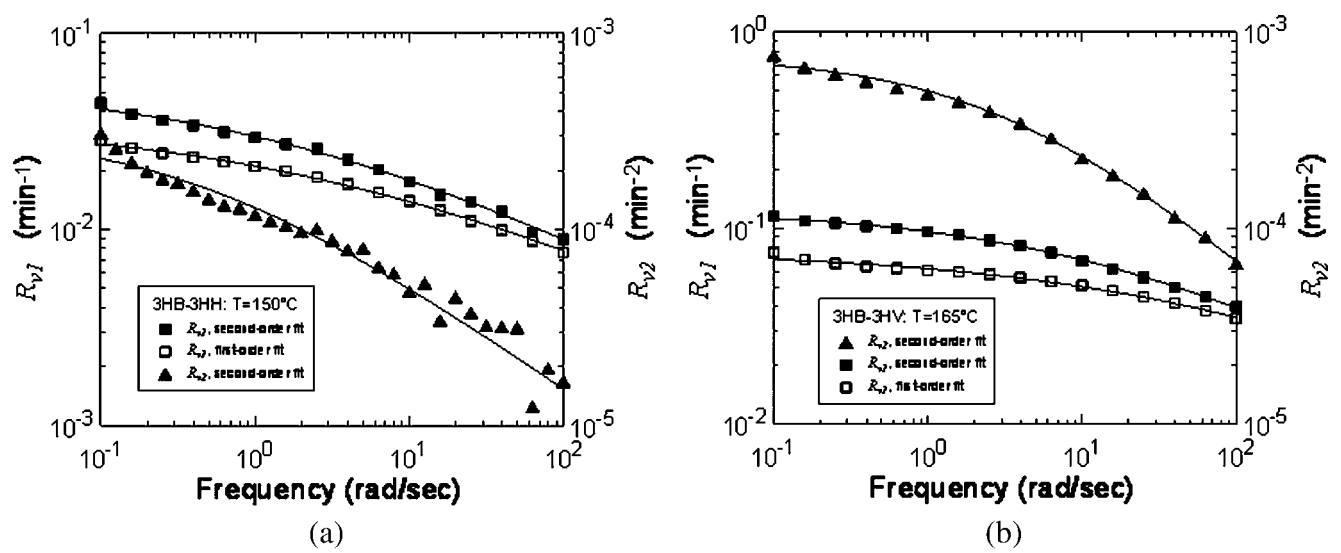

Figure 7 Viscosity loss rate behavior R_{vi} for (a) the 3HB-3HH copolymer and (b) the 3HB-3HV copolymer.

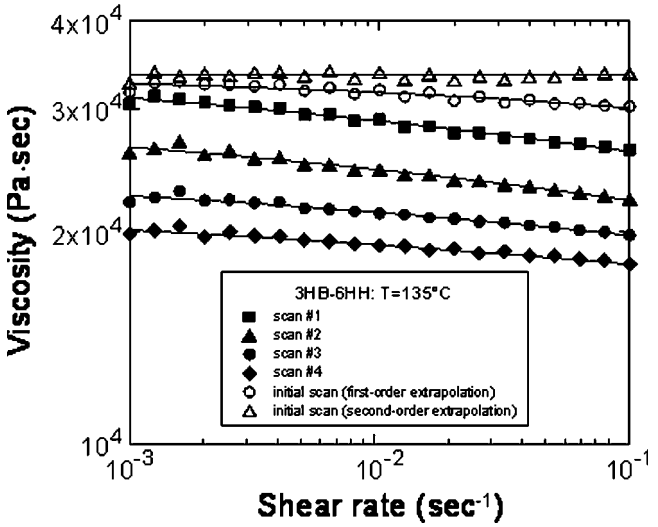

Figure 8 First-and second-order extrapolated shear viscosity–shear rate curves for the 3HB-6HH copolymer.

degradation) that are predicted by eq. (6). This figure shows the predicted values of the complex viscosity at all of the measured frequencies. Both the first-order extrapolation and the second-order extrapolation from eq. (6) are presented as open symbols. We note that at low frequencies, the second-order extrapolation predicts a slightly larger value of the complex viscosity than does the first-order extrapolation (as is expected from the results shown in Fig. 3), which is due to the form of eq. (5). However, at higher frequencies, the first- and second-order extrapolations collapse onto a single curve.

Also shown on Figure 4 are the Ellis model

$$\eta^* = \frac{\eta_0^*}{1 + (\tau\omega)^{1-n}}, \tag{8}$$

fits for each of the viscosity scans. In eq. (8), τ is a characteristic relaxation time and n is the power-law exponent. Use of the Ellis equation allows the fitting of a zero-shear value for the complex viscosity, although, for the time-dependent scans, it should be noted that this fitting does incorporate some time-dependent decrease in the viscosity due to degradation. However, at high frequencies, this time is relatively small due to the short time interval required for high frequency measurements.

In Figure 5, the time-dependent complex viscosities, at four representative frequencies, are shown for the 3HB-3HV copolymer, along with both the first- and second-order extrapolations determined using eq. (6). Here, more clearly, we see why the second-order extrapolation provides a better fit, especially at the low frequencies. Figure 6 shows the complex viscosity sweeps as a function of frequency, including both the complete first- and second-order extrapolations. Again, at high frequencies, the extrapolated curves collapse onto one another whereas, at low frequencies, the second-order extrapolation exceeds the first-order extrapolation in value. In addition, the sharp decrease in the experimental measured scans at low frequencies is eliminated with the second-order fit, because these decreases are due to the time required for the points to be measured experimentally (and therefore of the polymer degradation), rather than characteristic of the polymer rheology. It is interesting to note that the poorer fit offered by the first-order extrapolation does not eliminate this initial decrease.

The viscosity curves that are extrapolated to time zero, and therefore prior to degradation, depend on the viscosity loss rates R_{vi} defined by eq. (7). Figures 7(a) and 7(b) show the values of the R_{vi} for the 3HB-3HH and the 3HB-3HV copolymers, respectively. Values are shown for both the first- and second-order extrapolations. Given the form of eq. (6) with the alternating positive and negative terms, it is apparent that R_{v2} for the second-order fit should exceed R_{v1} for the first-order fit, and this is indeed the case. As expected, R_{v2} for the second-order fit is significantly lower in magnitude than the initial term. Equation (7) also enables one to determine the degradation rate constant k for each of the polymers. We find that a single value of k is valid for each of the polymers over the entire range of frequencies investigated.

Steady shear viscosity

Given the successes encountered with the complex viscosity results for two different polymers, we now seek to apply this model to the time-dependent steady shear rate sweeps shown for the 3HB-6HH

TABLE II
Zero-Shear Viscosities and Degradation Rate Constants for the 3HB-6HH Copolymer in Both Dynamic and Steady Testing, at a Test Temperature of 135°C

	Steady mode		Dynamic mode	
Analysis method	$\eta_0\|_{t=0}$ (10^4 Pa s)	k (10^{-7} min^{-1})	$\eta_0^*\|_{t=0}$ (10^4 Pa s)	k (10^{-6} min^{-1})
First-order extrapolation	3.37	9.05	3.15	1.16
Second-order extrapolation	3.34	1.3	3.44	1.71

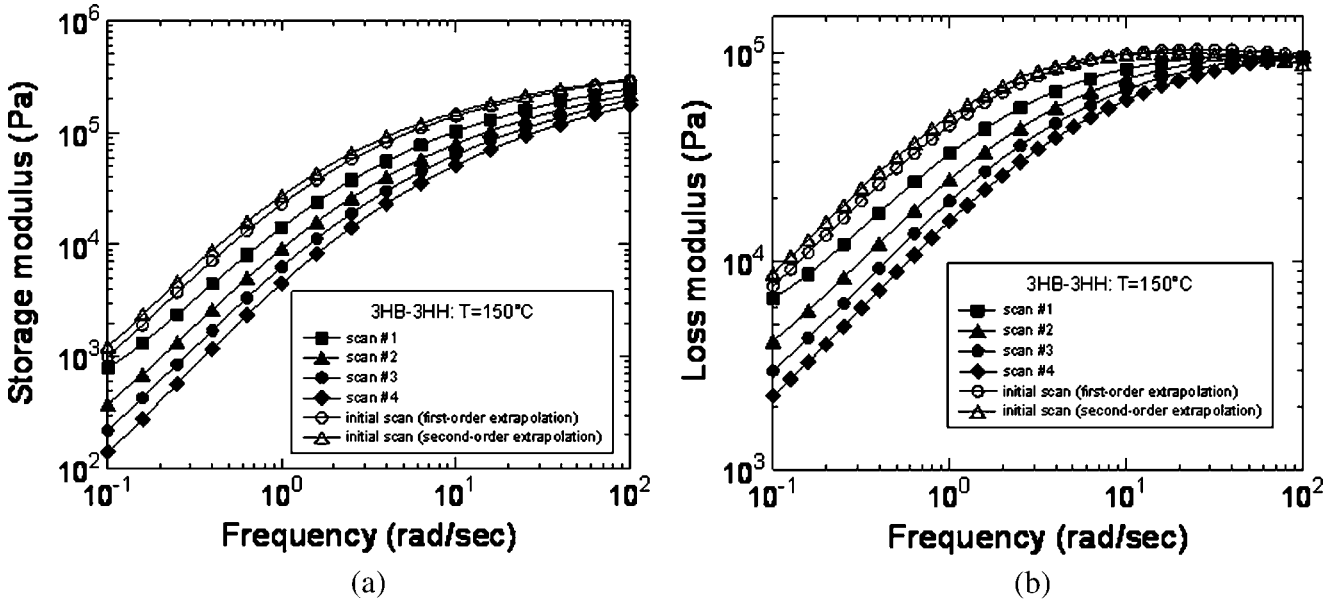

Figure 9 First-and second-order extrapolated moduli–frequency curves for the 3HB-3HH copolymer. (a) storage modulus $G'(\omega)$; (b) loss modulus $G''(\omega)$.

copolymer shown in Figure 2(b). Figure 8 shows the viscosity curves extrapolated to zero time in the absence of degradation. As expected, these results demonstrate the existence of the zero-shear viscosity plateau over the entire range of shear rates probed experimentally. Table II provides a comparison of the extrapolated viscosity curves for 3HB-6HH for both steady and dynamic testing. We note that the extrapolated values confirm the validity of the Cox–Merz rule for this material, and also note that the degradation constant k obtained in both types of experiment are of similar magnitude.

Dynamic moduli

The storage, $G'(\omega)$ and loss, $G''(\omega)$ moduli obtained from dynamic oscillatory experiments can provide significant information about the polymer under consideration. In this section, we attempt to extend the analysis presented earlier toward obtaining extrapolated time zero curves for the storage and loss moduli prior to polymer degradation. The complex viscosity $\eta^*(\omega)$ was actually calculated from the G' and G'' data, according to the following expression:

$$\eta^* = \frac{\sqrt{(G')^2 + (G'')^2}}{\omega}. \quad (9)$$

However, there is no general appropriate expression analogous to eq. (2) that relates the storage or loss moduli to molecular weight. Hence, there is no strong theoretical basis from which to develop an expression analogous to eq. (6). Instead, given that the complex viscosity η^* depends on the moduli as shown in eq. (9), we simply choose to assume that the moduli $G'(\omega)$ and $G''(\omega)$ follow a similar form to eq. (6) so that

$$\log G'(\omega, t) = \log G'(\omega)|_{t=0} + \sum_{i=1}^{\infty} (-1)^i (R_{G',i} t^i), \quad \text{and} \quad (10a)$$

$$\log G''(\omega, t) = \log G''(\omega)|_{t=0} + \sum_{i=1}^{\infty} (-1)^i (R_{G'',i} t^i). \quad (10b)$$

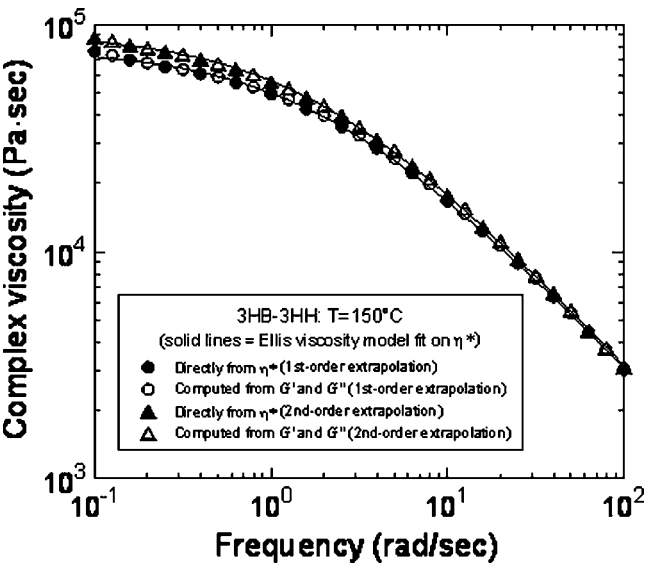

Figure 10 Extrapolated complex viscosity–frequency curves for the 3HB-3HH directly from η^* and computed using extrapolated values of G', G''.

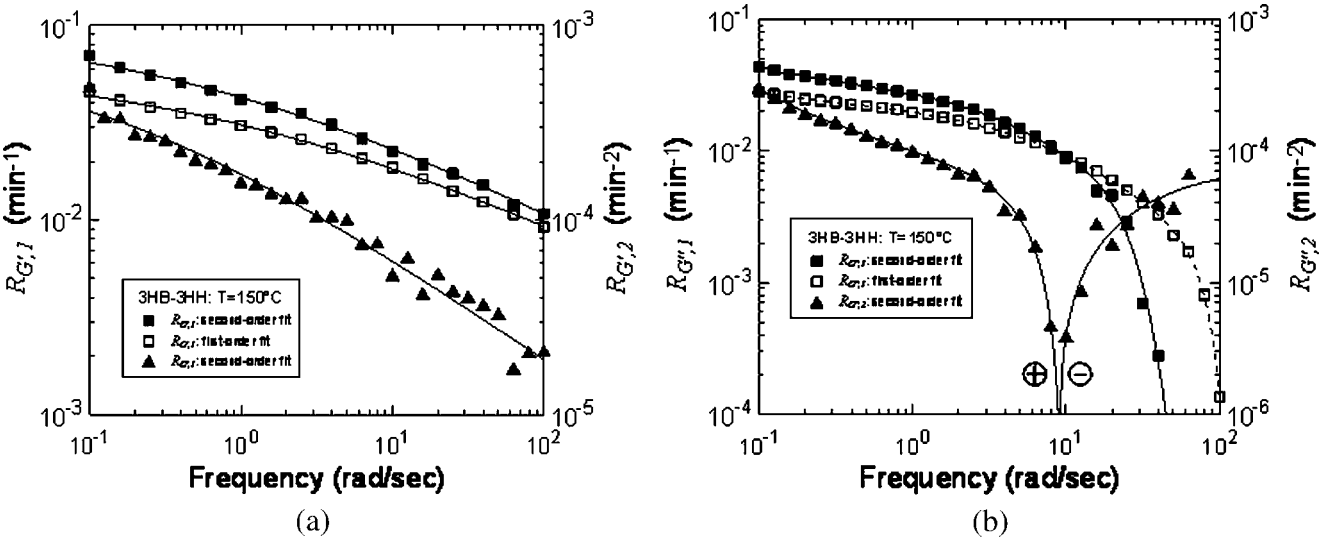

Figure 11 Loss rate behavior for the dynamic moduli for the 3HB-3HH copolymer. (a) $R_{G',i}$ and (b) $R_{G'',i}$.

Then, we use the first- and second-order extrapolation procedure to obtain the time zero curves as a function of frequency. Although the *ad hoc* form for the moduli is that of eq. (6) the *i*th-order loss rates $R_{G',i}$ and $R_{G'',i}$ are not the same as the R_{vi} terms found for the viscosity curves, and indeed we do not prescribe any physical significance to the values of $R_{G',i}$ and $R_{G'',i}$, which are determined for the moduli.

Figures 9(a) and 9(b) show the storage and loss moduli for the 3HB-3HH copolymer, along with the first- and second-order extrapolated values obtained using eqs. (10a) and (10b). As before, the second-order extrapolations result in a slightly larger value of G' and G'' than does the first order extrapolation. One way to evaluate the effectiveness of this *ad hoc* procedure for G' and G'' is to calculate the time zero complex viscosity $\eta^*(\omega)$, using the results from eqs. (10a) and (10b), and compare these results to those obtained, from a more theoretically rigorous analysis, from eq. (6). Figure 10 shows a remarkable agreement between these two methods.

We now turn to a discussion of the *ad hoc* loss rates $R_{G',i}$ and $R_{G'',i}$ obtained through the G' and G'' analysis. Figures 11(a) and 11(b) show, for the 3HB-3HH copolymer, the first- and second-order fit terms for the storage and loss modulus, respectively. For the storage modulus, the dependence on frequency is similar to that of eq. (3). However, the results for the loss modulus are qualitatively different and, above a certain frequency, the $R_{G'',2}$ term actually goes negative. Physically, this is inconsistent with the arguments presented for the viscosity expansion, and reinforces the notion that, although Figure 10 provides some support for the method, the analysis for the moduli is *ad hoc*.

One parameter that can be extracted from the dynamic moduli is the molecular weight between entanglements, M_e. This parameter describes the average molecular weight that occurs between entanglement points, and according to Doi–Edwards[21] theory this may be determined from

$$\tau_d = \frac{15}{\pi^2}\frac{\eta_0^*}{G_N^0} = \frac{15}{\pi^2}\frac{\eta_0^* M_e}{\rho RT}. \tag{11}$$

In eq. (11) G_N^0 is the plateau modulus and τ_d is the characteristic disengagement time may be approximated as $1/\omega_c$, where ω_c is the crossover frequency from linear viscoelastic measurements. Table III provides values for M_e for the three different copolymers under consideration. Because 3HB-6HH has the most flexible chain backbone due to the linear 6HH monomer, its M_e is the lowest of the copolymers investigated. Although the 3HH monomer results in a longer side chain than does the 3HV monomer, we find that the 3HB-3HH has a lower M_e than 3HB-3HV. This may be attributed to the lower comonomer concentration for the 3HB-3HH copolymer and the isotacticity of the 3HB-3HV.

TABLE III
Estimated Molecular Weights between Entanglements for the Copolymers, Based upon Experiments Performed at the Indicated Temperatures

Analysis method	3HB-3HV (T = 165°C)	3HB-3HH (T = 150°C)	3HB-6HH (T = 135°C)
First-order extrapolation	12,800	7800	6000
Second-order extrapolation	13,600	7700	5700

CONCLUSIONS

A theoretical framework has been developed that enables one to better quantify the rheology and initial physical properties of polymer materials that degrade over the time interval required for experimental characterization. Based upon a fundamental understanding of the degradation kinetics, the complete flow curves can be determined for a time prior to degradation. The parameters that can be determined include a characteristic relaxation time and the molecular weight between entanglements.

The method is applied to both time-dependent complex viscosity–frequency data and the time-dependent steady shear viscosity-shear rate data for three different PHA copolymers. A time zero flow curve may be obtained with either a first- or a second-order extrapolation procedure. On the basis of the extrapolated curves, the Cox–Merz rule is confirmed. A degradation rate constant k can also be determined, that is valid over the entire range of frequencies/shear rates investigated.

In addition to the time zero extrapolated viscosity curves, a similar method is applied to the raw storage and loss moduli data. Although this method is clearly *ad hoc*, given the absence of an appropriate relationship between the moduli and molecular weight, a comparison between the curves obtained directly from extrapolated complex viscosity data and those obtained using extrapolated G' and G'' data indicates that the values obtained are reasonable.

References

1. Doi, Y. Microbial Polyesters; VCH: Weinheinn, 1990.
2. Hartmann, M. H. In Biopolymers from Renewable Resources; Kaplan, D. L., Ed., Springer-Verlag: Berlin, 1998.
3. Luzier, W. D. Proc Natl Acad Sci USA 1992, 89, 839.
4. Holmes, P. A. Phys Teach 1985, 16, 32.
5. Bauer, H.; Owen, A. J. Colloid Polym Sci 1989, 266, 241.
6. Kunioka, M.; Kawagushi, Y.; Doi, Y. Appl Microbiol Biotechnol 1989, 30, 569.
7. Kunioka, M.; Tamaki, A.; Doi, Y. Macromolecules 1989, 22, 694.
8. Melik, D. H.; Schechtman, L. A. Polym Eng Sci 1995, 35, 1795.
9. Gursel, I.; Balcik, C.; Arica, Y.; Akkus, O.; Akkas, N.; Hasirci, V. Biomaterials 1998, 19, 1137.
10. Matsusaki, H.; Abe, H.; Doi, Y. Biomacromolecules 2000, 1, 17.
11. Baltieri, R. C.; Mei, L. H. I.; Bartoli, J. Macromol Symp 2003, 197, 33.
12. Dias, M. L.; Giornes, A. M.; Mendes, L. C. Polym Polym Compos 2003, 11, 189.
13. Zhao, K.; Deng, Y.; Chen, J. C.; Chen, G. Q. Biomaterials 2003, 24, 1041.
14. Satkowski, M. M.; Melik, D. H.; Autran, J.-P.; Green, P. R.; Noda, I.; Schechtman, L. A. In Biopolymers Polyesters. II. Properties and Chemical Synthesis; Doi, Y., Steinbuchel, A., Eds.; Wiley-VCH: New York, 2002; Vol. 3b.
15. Daly, P. A.; Bruce, D. A.; Melik, D. H.; Harrison, G. M. J Appl Polym Sci 2005, 98, 64.
16. Jellineck, H. H. G.; Chaudhuri, A. K. J Polym Sci A-1: Polym Chem 1972, 10, 1773.
17. Tharmapuram, S. R.; Jabarin, S. A. Adv Polym Tech 2003, 22, 147.
18. Cox, W. P.; Merz, E. H. J Polym Sci 1958, 28, 619.
19. Lehrle, R. S.; Williams, R. J. Macromolecules 1994, 27, 3782.
20. Seo K. S.; Cloyd J. D. J Appl Polym Sci 1991, 42, 845.
21. Doi, M.; Edwards, S. F. The Theory of Polymer Dynamics; Oxford University Press: Oxford, 1986.